Treatment of aortic stenosis with aortic valve bypass (apicoaortic conduit) surgery: An assessment using computational modeling

Elias Balaras, PhD,[a] K. S. Cha, PhD,[a] Bartley P. Griffith, MD,[b] and James S. Gammie, MD[b]

Background: Aortic valve bypass surgery treats aortic valve stenosis with a valve-containing conduit that connects the left ventricular apex to the descending thoracic aorta. After aortic valve bypass, blood is ejected from the left ventricle via both the native stenotic aortic valve and the conduit. We performed computational modeling to determine the effects of aortic valve bypass on aortic and cerebral blood flow, as well as the effect of conduit size on relative blood flow through the conduit and the native valve.

Methods: The interaction of blood flow with the vascular boundary was modeled using a hybrid Eurelian–Lagrangian formulation, where an unstructured Galerkin finite element method was coupled with an immersed boundary approach.

Results: Our model predicted native (stenotic) valve to conduit flow ratios of 45:55, 52:48, and 60:40 for conduits with diameters of 20, 16, and 10 mm, respectively. Mean gradients across the native aortic valve were calculated to be 12.5, 13.8, and 17.6 mm Hg, respectively. Post–aortic valve bypass cerebral blood flow was unchanged from preoperative aortic valve stenosis configurations and was constant across all conduit sizes. In all cases modeled, cerebral blood flow was completely supplied by blood ejected across the native aortic valve.

Conclusions: An aortic valve bypass conduit as small as 10 mm results in excellent relief of left ventricular outflow tract obstruction in critical aortic valve stenosis. The presence of an aortic valve bypass conduit has no effect on cerebral blood flow. All blood flow to the brain occurs via antegrade flow across the native stenotic valve; this configuration may decrease the long-term risk of cerebral thromboembolism.

Surgical aortic valve replacement (AVR) improves quality of life and extends survival in most patients with symptomatic aortic stenosis (AS). Although isolated AVR can be performed with an acceptable operative mortality,[1,2] the requirement for cardiopulmonary bypass, median sternotomy, aortic crossclamping, valve debridement, and cardioplegic cardiac arrest confers risks of morbidity and mortality to patients undergoing conventional AVR. These risks are particularly acute in high-risk subpopulations including the elderly and patients with previous cardiac surgery, cerebrovascular disease, and concomitant calcific aortic disease.[2-4] There is growing evidence that the majority of patients with symptomatic AS are never considered for surgery as a result of real and perceived risks of conventional AVR, despite the fact that unoperated symptomatic AS carries a dismal prognosis.[5]

Aortic valve bypass (AVB) surgery is an alternative to conventional aortic valve replacement and can extend the benefits of surgical relief of aortic stenosis to high-risk AS populations. AVB surgery relieves the left ventricular outflow obstruction of aortic stenosis through the construction of a second outflow tract from the left ventricle. A Dacron conduit containing a bioprosthetic valve originates at the left ventricular apex and terminates at a right angle to the descending thoracic aorta (Figure 1). Potential advantages of AVB compared with conventional AVR include avoidance of (redo) sternotomy in the presence of patent coronary bypass grafts; avoidance of aortic crossclamping, cardiopulmonary bypass, and cardioplegic arrest; and a low likelihood of postoperative heart block and patient–prosthesis mismatch.[6] Although AVB is known to be a durable operation, with some patients surviving more than 24[7] and 25 (personal communication, John W. Brown) years, to date the circulatory physiology of AS treated with an AVB conduit has been poorly characterized. We have now used computational fluid dynamic (CFD) modeling to answer key questions about the circulatory system after AVB surgery. The goals of this study were to answer the following questions: (1) What is the relative blood flow through the native stenotic valve and the conduit, and what are the key determinants of this distribution? (2) Does AVB surgery relieve the left ventricular outflow tract obstruction of critical AS? (3) Does CFD modeling accurately predict gradients across the native (stenotic) aortic valve after AVB surgery? (4) Is cerebral blood flow supplied from antegrade flow through the native aortic valve, via the conduit, or a combination of both? (5) Is cerebral

From the Department of Mechanical Engineering[a] and Division of Cardiac Surgery,[b] University of Maryland Medical Center, Baltimore, Md.

Received for publication May 2, 2008; revisions received July 17, 2008; accepted for publication Aug 19, 2008.

Address for reprints: James S. Gammie, MD, Division of Cardiac Surgery, University of Maryland Medical Center, N4W94, 22 South Greene Street, Baltimore, MD 21201 (E-mail: jgammie@smail.umaryland.edu).

J Thorac Cardiovasc Surg 2009;137:680-7
0022-5223/$36.00

doi:10.1016/j.jtcvs.2008.08.032

Abbreviations and Acronyms
ALE = arbitrary Lagrangian-Eulerian
AS = aortic stenosis
AVB = aortic valve bypass
AVR = aortic valve replacement

blood flow unchanged after the treatment of AS with an AVB?

METHODS

Problem Formulation and Numerical Method

To investigate the extensive parametric space that directly affects the local blood flow after AVB surgery, we performed a series of computations on an idealized 2-dimensional configuration of the heart and great vessels. A sketch of the geometry is shown in Figure 2. The model includes an idealization of the left ventricle followed by a curved channel that represents the aortic arch. The brachiocephalic, left common carotid, and left subclavian arteries arise from the aortic arch. The mitral, aortic, and conduit valves are included and are represented by plates with 0 thickness. Blood flow is driven by the motion of the ventricular walls. The dimensions of the overall setup, including the conduit, are representative of a typical clinical scenario and are based on clinical experience and measurements in normal subjects.[6]

The fluid flow in the left ventricle and the surrounding vessels is governed by the Navier-Stokes equations:

$$\nabla \cdot u = 0 \tag{1}$$

$$\frac{\partial u}{\partial t} + \tilde{u} \cdot \nabla u = -\nabla_p + v\nabla^2 u + f, \tag{2}$$

where u is the velocity vector, p is the pressure normalized by the fluid density, v is the kinematic viscosity, f is a body force term, and $\tilde{u} = u - u_g$ is the fluid velocity relative to a grid moving with velocity, u_g. To solve Equations (1) and (2) for the geometry given above, which includes complex moving boundaries, a hybrid ALE (arbitrary Lagrangian-Eulerian)/immersed boundary formulation has been developed. The basic solver uses an ALE/finite-element formulation, which employs an efficient, explicit, fractional 4-step method allowing for the use of equal interpolation spaces for the pressure and velocity fields.[8] The spatial discretization is done using a Galerkin method, where an explicit Lax–Wendrof-type scheme is used for the convective terms to prevent checkerboard pressure oscillations. Details on the overall formulation and its validation for a variety of prototypical fluid and fluid–structure interaction problems can be found in Cha[8] and Balaras.[9] The above solver works well on complex geometries with relatively small boundary motion but may become inefficient in cases with very large displacements/deformations. The motion of the ventricular walls, for example, could be accommodated by simply deforming the grid to conform to the new location of the boundary at each time step. The motion of the valve leaflets on the other hand, which undergo large rotational displacements and come in contact with other stationary or moving boundaries, would require frequent regeneration of the overall grid. As a result, grid quality as well as accuracy and efficiency of the overall solver are difficult to preserve. To overcome this problem, the effect of the leaflet motion on the flow is introduced by an immersed boundary formulation. In such case, the requirement for the grid to conform to the moving boundary is relaxed, and the boundary conditions are enforced using a forcing function, f. The overall method is an extension of our previous work on immersed boundary methods for structured Cartesian and cylindrical coordinate grids to fully unstructured grids.[9,10] In the present implementation, an arbitrary, 2-dimensional, immersed body is represented by a series of Lagrangian marker particles. At each time step, the relation between the marker particles and the underline finite element grid is identified and the forcing function, f in Equation (2), is constructed in a way that the desired boundary conditions are satisfied. The overall approach maintains second-order accuracy in space and time.

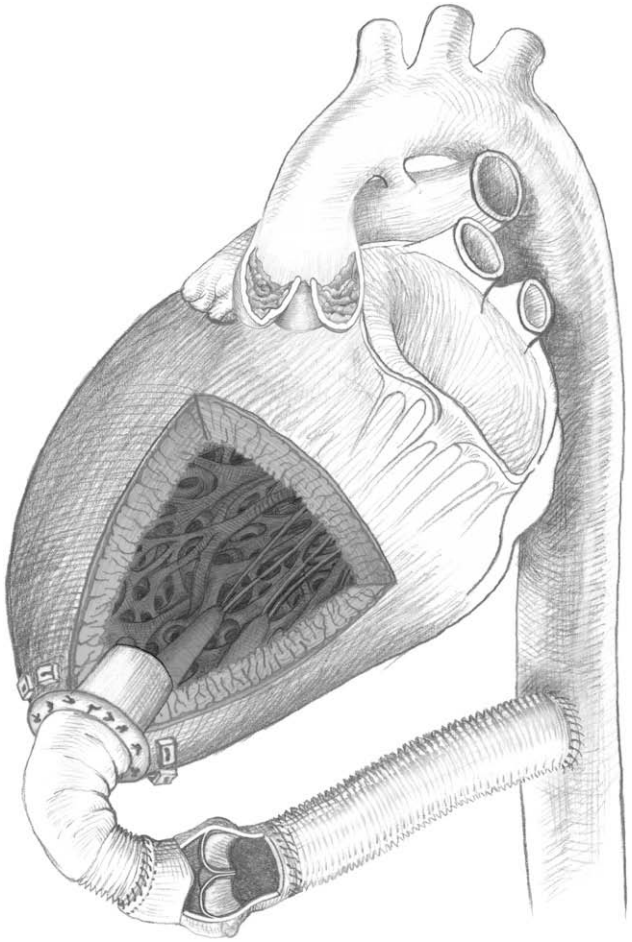

FIGURE 1. Aortic valve bypass.

Computational Setup and Parametric Space

The primary objective of the series of computations reported in the present study is to investigate how a valve-containing conduit implanted during AVB surgery impacts the overall flow patterns in the surrounding great vessels. We studied the following configurations: case I: normal; case II : severe AS; cases III–V: severe AS with AVB conduit diameters of 20, 16, and 10 mm, respectively (Table 1, Figure 2). The conduit valve was also scaled down by the same factor. Blood flow is driven by the simple harmonic motion of the ventricular walls. The motion of the valves is imposed and is based on earlier, highly detailed, fully 3-dimensional simulations of the flow past prosthetic valves.[10] A typical computational grid is shown in Figure 3 and consists of approximately 125,000 elements. The overall grid continuously deforms in order to conform to the moving ventricular walls. This requirement, however, is relaxed for the case of the valves, and their motion is introduced using the immersed boundary formulation discussed above. All vascular boundaries were assumed to be rigid for all calculations and the no-slip condition was applied.

In Figure 4, the ventricular motion during 1 cardiac cycle is shown together with the resulting flow rate through the aortic and mitral valves

ACD

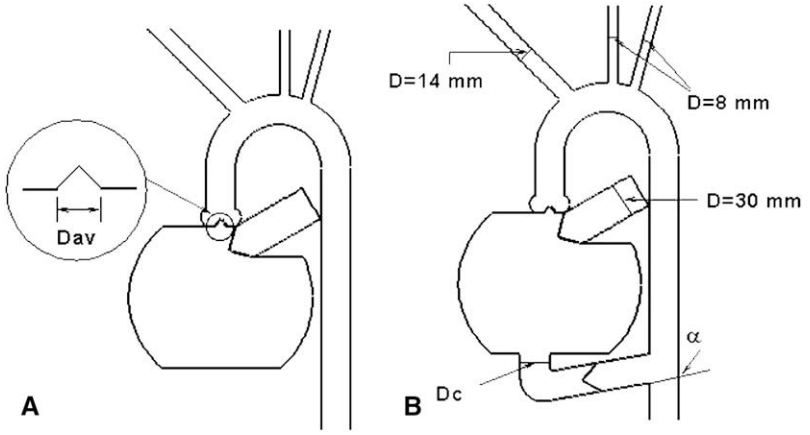

FIGURE 2. Simplified, 2-dimensional representation of the left ventricle and surrounding vessels. A, Reference configuration. *Dav,* Diameter of stenotic aortic valve orifice = 9 mm. B, Configuration after aortic valve bypass surgery for aortic stenosis. For all cases considered, $\alpha = 90^\circ$ and the diameters of the innominate, left carotid, subclavian, and mitral inflow tract are 14, 8, 8, and 30 mm, respectively.

and the valved conduit. The instant opening and closing time for each valve is also indicated in the figure. The simple harmonic motion of the ventricular wall allowed for a straightforward implementation of the valve kinematics and results in flow rate variations that are in broad qualitative agreement with the clinical data.

For all cases, the native aortic valve is assumed to have an 80% area stenosis. Assuming that a healthy valve has an area of approximately 3.5 cm^2, for example, an 80% area stenosis is equivalent to an aortic valve area of 0.65 cm^2. In all 4 configurations, a constant pressure boundary condition has been used. Blood is assumed to be a Newtonian fluid with density $\rho = 1.1$ g/cm^3 and viscosity $\nu = 0.035$ P. The pick Reynolds number (based on the average velocity, U_b, and the diameter of the aorta), a nondimensional number characterizing the relative importance of viscous to inertial effects, is approximately 4000. For all cases listed in Table 1, the computations were initialized with quiescent flow and integrated in time until a quasi-periodic state was reached and the effects of initial conditions were eliminated (typically 3 to 4 cycles). All results are presented for the cardiac cycles after this stage.

Echocardiography

Quantitative Doppler echocardiography was performed on all patients prior to hospital dismissal. Standardized evaluation included calculation of mean gradients across the native (stenotic) aortic valve and was performed in accordance with the American Society of Echocardiography's standardized reporting recommendations.[11] A total of 17 patients with 20-mm conduits were available for echocardiographic assessment.

RESULTS

In Table 2, the mean native aortic valve pressure gradients for the configurations considered are listed. Echocardiographically determined mean transvalvular gradients for patients with severe symptomatic AS are from reference values in the literature.[6] For consistency, we used the same approach used in echocardiography (the modified Bernoulli equation) to compute aortic valve pressure gradients.[12,13]

The mean velocity at the valve is computed by averaging the computed velocity in the cross-sectional area. In order to perform direct comparisons with the clinical data, all values in Table 2 are scaled to the corresponding gradient from the case of severe untreated AS. For severe AS (80% stenosis, aortic valve area = 0.65 cm^2) treated with a 20-mm AVB conduit, our model predicts a mean native (stenotic) aortic transvalvular gradient of 12.5 mm Hg. In our clinical experience to date with a 20-mm AVB conduit with a nominal-sized 21 stentless porcine bioprosthetic valve (n = 17), the mean native (stenotic) transvalvular gradient determined echocardiographically was 10.5 ± 6 mm Hg, which is within 19% of the value predicted from the computational model. When the diameter of the AVB conduit is decreased stepwise to 16 then to 10 mm, our simulations predict mean gradients of 13.8 and 17.6 mm Hg, respectively.

Figure 5 demonstrates blood flow through the native valve, the conduit, and the 3 aortic arch vessels for cases I to V. All flows are normalized to the peak systolic flow in case II, Q_o, which represents untreated severe aortic stenosis. For case III (severe AS treated with a 20-mm AVB conduit), the ratio of the total amount of blood flow through the native stenotic aortic valve during the cardiac cycle to that of the conduit is 45:55. As the conduit size is reduced in cases IV and V, the corresponding ratios are 52:48 and 60:40, respectively.

Blood flow to the 3 aortic arch vessels was minimally affected by the presence or size of the AVB conduit. In case II, for example, which represents untreated severe aortic stenosis, peak blood flow through the brachiocephalic, left

TABLE 1. Summary of the computations

Case	Native aortic valve stenosis (%)	Diameter of AVB conduit, *D* (mm)
I, Normal	0	No conduit
II, AS	80	No conduit
III, AS + 20 mm AVB	80	20
IV, AS + 16 mm AVB	80	16
V, AS + 10 mm AVB	80	10

AS, Aortic stenosis; *AVB,* aortic valve bypass; *D,* diameter.

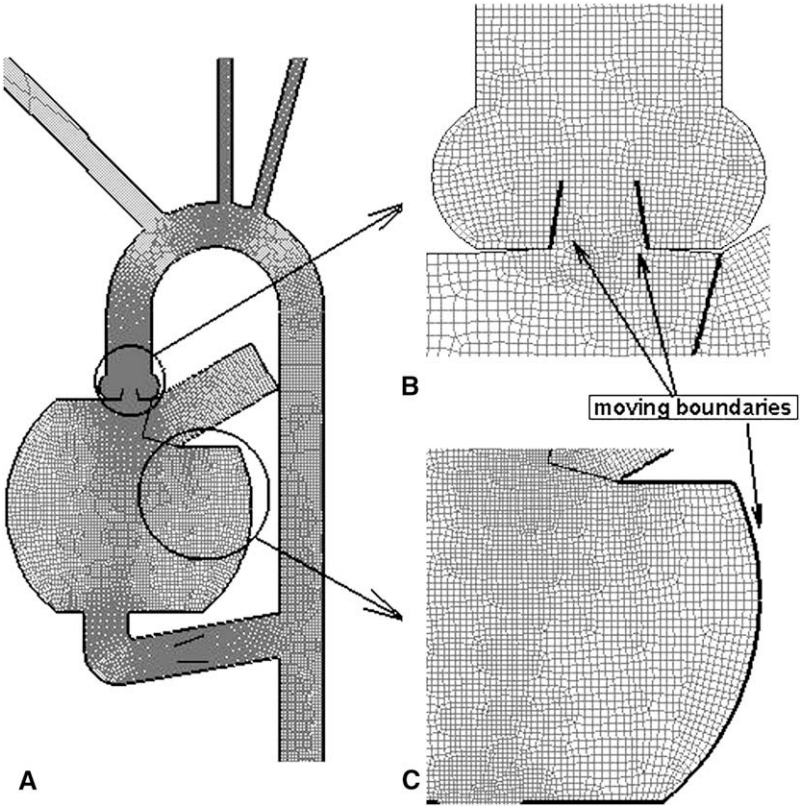

FIGURE 3. A, Snapshot of the computational grid (only a fraction of the grid points are plotted for clarity) for case II. B, Detail of the grid around the aortic valve. Notice that the grid does not follow the surface valve. C, Detail of the grid around the moving part of the ventricular boundary.

carotid, and subclavian arteries was $0.29Q_o$, $0.18Q_o$, and $0.18Q_o$, respectively. For all cases with the AVB conduit, the corresponding flow rates were unchanged (flow variation less than 3% from reference).

In Figure 6, instantaneous flow patterns and velocities for cases II (untreated aortic stenosis), III (20-mm conduit), and V (10-mm conduit) are compared during peak systole. Isocontours of the V velocity component (along the axis of the descending aorta) are shown. In all cases, a strong jet through the native stenotic aortic valve can be observed. As expected and consistent with our hypothesis that the presence of an AVB conduit relieves the left ventricular outflow tract obstruction of AS, the jet velocity decreases substantially after insertion of the AVB conduit: the maximum velocity is $0.51U^{\mathrm{II}}{}_{\max}$ (where $U^{\mathrm{II}}{}_{\max}$ is the maximum velocity in case II, untreated aortic stenosis) and $0.62U^{\mathrm{II}}{}_{\max}$ for cases III and V, respectively. The velocity magnitude in the middescending aorta is also affected, and in all post-AVB cases, it is approximately 6 to 7 times smaller compared with the untreated aortic stenosis model. For the 2 cases with the larger conduit size (cases III and IV), there is also some flow reversal in the descending aorta immediately cephalad to the distal insertion of the AVB conduit as seen in the inserts at the lower part of Figure 6. This can be seen more clearly in Figure 7 where flow patterns in the region of the distal anastomosis are shown. For case III (20-mm AVB conduit), there is reversal of flow in the descending aorta immediately cephalad to the distal insertion of the AVB, with a small proportion of conduit flow directed upward in the descending aorta, and for case V (10-mm conduit), the flow coming from the native valve merges with the one coming out of the conduit and no flow reversal is observed. The 20-mm conduit model is consistent with our clinical experience, where we have observed flow reversal patterns similar to those created with this model on postoperative magnetic resonance imaging. In our CFD model, all blood flow to the brain (ie, flow to the innominate and left carotid arteries) is completely supplied from antegrade flow across the stenotic aortic valve, even in the presence of a large (20-mm diameter) AVB conduit.

DISCUSSION

Although AVB surgery has been performed clinically for more than 50 years, there have been no efforts to characterize the circulatory physiology after insertion of a valved conduit from the apex of the left ventricle to the descending aorta. The present investigation, using sophisticated CFD modeling, has allowed us to answer some basic questions about the nature and determinants of the circulation after

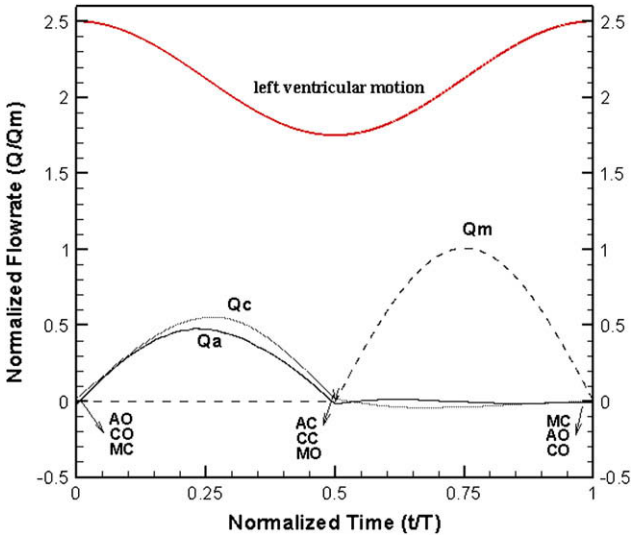

FIGURE 4. Imposed displacement of the ventricular walls during 1 cardiac cycle. Also shown are the resulting flow rates through the native aortic valve *(Qa)*, conduit *(Qc)*, and mitral valve *(Qm)*. All flow rates are normalized with the peak flow rate through the mitral valve, and time with the duration of the cardiac cycle. The opening and closing times for all 3 valves are also indicated in the figure. *AO*, Opening of the aortic valve; *AC*, closing of the aortic valve; *CO*, opening of the conduit valve; *CC*, closing of the conduit valve; *MO*, opening of the mitral valve; *MC*, closing of the mitral valve.

AVB surgery. Our studies have demonstrated that insertion of a valved conduit from the apex of the left ventricle to the descending thoracic aorta results in highly effective relief of left ventricular outflow tract obstruction. The predicted mean gradient across the native (stenotic) aortic valve after insertion of an AVB conduit in our model (with a 20-mm diameter AVB conduit) was 12.5 mm Hg, which is remarkably close to the echocardiographically determined value of 10.5 $\pm$ 6.0 mm Hg as measured in 17 clinical cases. These values compare favorably to gradients measured across bioprosthetic and mechanical replacement valves after clinically successful conventional aortic valve replacement surgery and reinforce our clinical perception that AVB surgery results in reliable symptom relief and prolongation of survival.[14-18]

AVB surgery results in 2 outflow tracts for egress of blood from the left ventricle. Adequacy of cerebral blood flow is a frequent concern when this approach is considered. The present studies demonstrate no appreciable change in cerebral blood flow (ie, through the innominate and left carotid arteries) in all AVB configurations modeled. Because cerebral blood flow is a function of resistance in the cerebral circulation and pressure in the aorta and aortic pressure is normal after AVB surgery, these results are not surprising.

The long-term risk of stroke after conventional aortic valve replacement surgery is a significant concern and is of particular importance in younger patients as that risk is amortized over the individual's lifetime. Both mechanical and bioprosthetic aortic valves are associated with thromboembolism risk between 0.5% and 2.0% per year.[19] At 15-year follow-up, approximately 20% of patients having aortic valve replacement had suffered a stroke in 1 large study.[20] In our clinical experience, thromboembolism is very uncommon in midterm follow-up after AVB surgery, despite a population at very high risk of stroke. We hypothesize that AVB surgery confers protection from stroke because all blood flow to the brain is directed across the native (stenotic) valve, rather than across a prosthesis as is the case after conventional AVR. Thrombus that forms on the bioprosthesis cannot embolize to the brain. These computational fluid dynamic modeling studies support this hypothesis: in all cases examined, blood flow to the brain was antegrade across the native (stenotic) aortic valve. Even in case II (conduit size 20 mm), where the most significant flow reversal in the descending aorta occurs, all blood flow to the innominate and left carotid arteries was supplied in an antegrade fashion.

As we decreased the size of the AVB conduit in our model, we found that it had a relatively small effect on the gradient across the native (stenotic) valve. Reduction of the diameter from 20 mm to 10 mm, for example, increased the gradient across the native valve by 25% (mean gradient increased from 12.5 mm Hg to 17.6 mm Hg). This value is still well below that of untreated aortic stenosis, suggesting that a smaller conduit compared to that which is currently used in clinical practice might be adequate to treat aortic stenosis.

Due to the number of approximations involved in our model, care must be taken in relating these results to clinical practice. The curvature of the conduit, size and type of valve, angle of proximal and distal anastomosis, degree of aortic insufficiency, and cardiac output are among the parameters

TABLE 2. Native aortic valve gradients

	Clinical data		Numerical data (2-D)	
	Mean (mm Hg)	Mean normalized	Mean (mm Hg)†	Mean normalized
Case II (80% stenosis)	43.0 $\pm$ 7.0*	1	43.0	1
Case III (AVB, D = 20 mm)	10.5 $\pm$ 6.0*	0.24	12.5	0.29
Case IV (AVB, D = 16 mm)	—	—	13.8	0.32
Case V (AVB, D = 10 mm)	—	—	17.6	0.41

AVB, aortic valve bypass; *D*, diameter. *From Gammie et al.[6] †The numerical data are simply rescaled using the untreated native stenotic valve gradient as a reference.

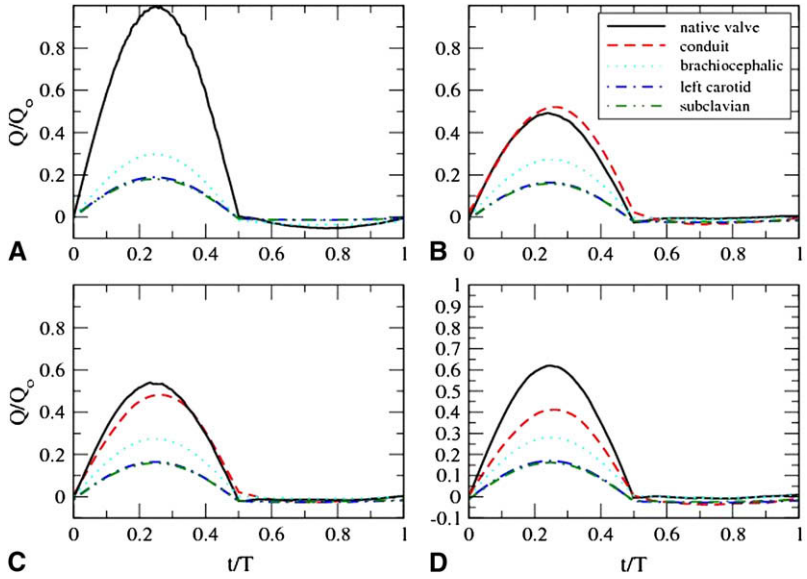

FIGURE 5. Relative blood flow through the native valve, the conduit, and the 3 aortic arch vessels as a function of time. A, Case II (untreated severe aortic stenosis). B, Case III (severe aortic stenosis with aortic valve bypass [AVB] conduit diameter 20 mm). C, Case IV (severe aortic stenosis with AVB conduit diameter 16 mm). D, Case V (severe aortic stenosis with AVB conduit diameter 10 mm). All flows are normalized to the peak value from case II.

that can influence this outcome and have not been incorporated in the present 2-dimensional model. Further 3-dimensional experimental and numerical studies are necessary to provide more precise quantitative answers regarding the ideal conduit diameter, size, shape, and anastomosis location.

These CFD studies have characterized the circulatory physiology after AVB surgery. We have demonstrated

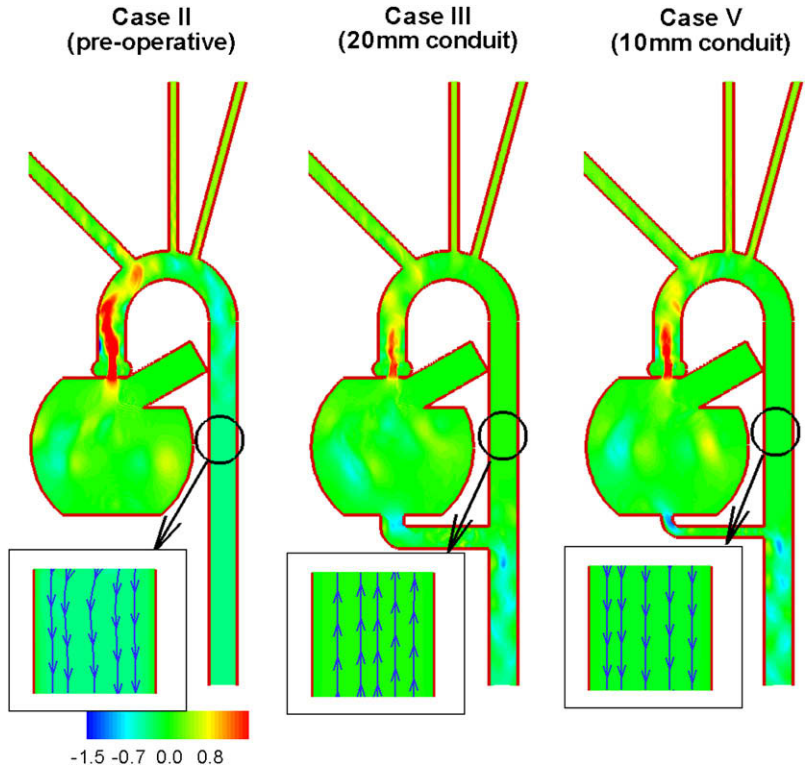

FIGURE 6. Snapshot of peak systolic flow. Isolines of the velocity component along the y-axis (axis aligned with descending aorta) are shown. The *insert* in each case shows streak lines indicating the flow direction.

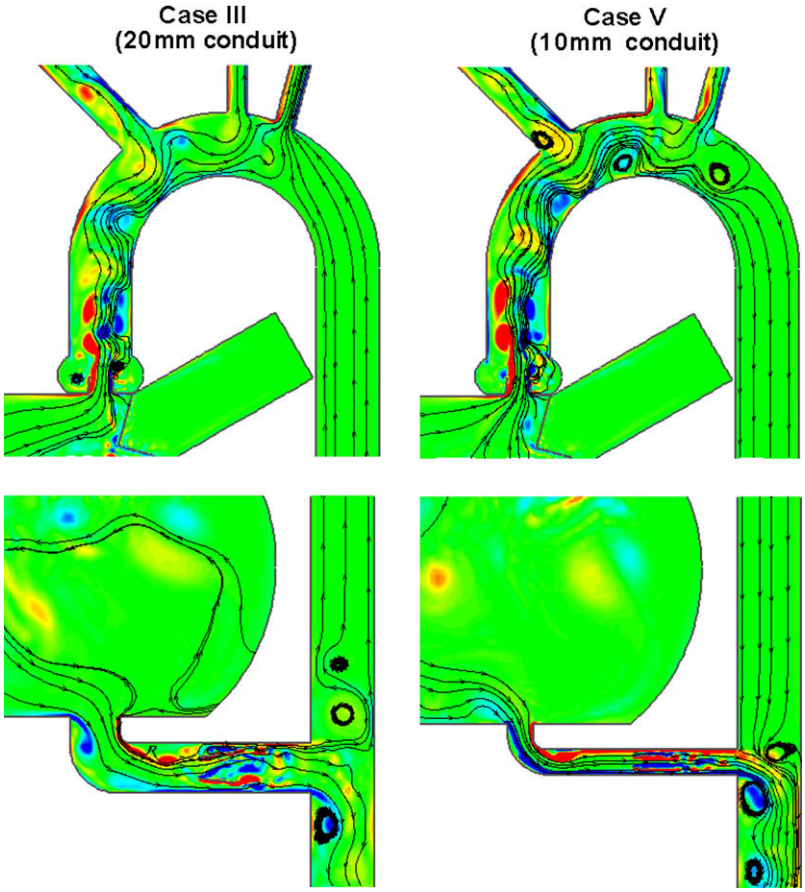

FIGURE 7. Snapshot of the flow at peak systole. Isolines of the vorticity are shown. Superimposed are stream traces indicating the flow direction.

that AVB conduit insertion effectively relieves native aortic valve stenosis, that cerebral blood flow is quantitatively unchanged after placement of an AVB, that all cerebral blood flow arises from the native left ventricular outflow tract, and that smaller conduit diameters than currently used clinically are associated with adequate relief of aortic stenosis.

References

1. Tabata M, Umakanthan R, Cohn LH, Bolman RM 3rd, Shekar PS, Chen FY, et al. Early and late outcomes of 1000 minimally invasive aortic valve operations. *Eur J Cardiothorac Surg*. 2008;33:537-41.
2. Bloomstein LZ, Gielchinsky I, Bernstein AD, Parsonnet V, Saunders C, Karanam R, et al. Aortic valve replacement in geriatric patients: determinants of in-hospital mortality. *Ann Thorac Surg*. 2001;71:597-600.
3. Varadarajan P, Kapoor N, Bansal RC, Pai RG. Survival in elderly patients with severe aortic stenosis is dramatically improved by aortic valve replacement: results from a cohort of 277 patients aged > or =80 years. *Eur J Cardiothorac Surg*. 2006;30:722-7.
4. Byrne JG, Karavas AN, Filsoufi F, Mihaljevic T, Aklog L, Adams DH, et al. Aortic valve surgery after previous coronary artery bypass grafting with functioning internal mammary artery grafts. *Ann Thorac Surg*. 2002;73:779-84.
5. Charlson E, Legedza AT, Hamel MB. Decision-making and outcomes in severe symptomatic aortic stenosis. *J Heart Valve Dis*. 2006;15:312-21.
6. Gammie JS, Brown JW, Brown JM, Poston RS, Pierson RN 3rd, Odonkor PN, et al. Aortic valve bypass for the high-risk patient with aortic stenosis. *Ann Thorac Surg*. 2006;81:1605-10.
7. Freeman LJ, de Leval MR, Tsang VT. The longest functioning apical left ventricular to descending aortic valve conduit. *Ann Thorac Surg*. 2005;79:1420.
8. Cha KS.Finite element analysis of unsteady separated flows around a moving body. PhD thesis. Chonnam National University: Gwangju, South Korea; 2004.
9. Balaras E. Modeling complex boundaries using an external force field on fixed Cartesian grids in large-eddy simulations. *Computers & Fluids*. 2004;33:375-404.
10. Yang JM, Balaras E. An embedded-boundary formulation for large-eddy simulation of turbulent flows interacting with moving boundaries. *J Comput Phys*. 2006;215:12-40.
11. American Society of Echocardiography. Recommendations for a standardized report for adult transthoracic echocardiography. Available at www.asecho.org/14a/pages/index.cfm?pageid=3317. Accessed October 8, 2008.
12. Callahan MJ, Tajik AJ, Su-Fan Q, Bove AA. Validation of instantaneous pressure gradients measured by continuous-wave Doppler in experimentally induced aortic stenosis. *Am J Cardiol*. 1985;56:989-93.
13. Hegrenaes L, Hatle L. Aortic stenosis in adults. Non-invasive estimation of pressure differences by continuous wave Doppler echocardiography. *Br Heart J*. 1985;54:396-404.
14. Dalmau MJ, Maria Gonzalez-Santos J, Lopez-Rodriguez J, Bueno M, Arribas A, Nieto F. One year hemodynamic performance of the Perimount Magna pericardial xenograft and the Medtronic Mosaic bioprosthesis in the aortic position: a prospective randomized study. *Interact Cardiovasc Thorac Surg*. 2007;6:345-9.
15. Tasca G, Brunelli F, Cirillo M, Dalla Tomba M, Mhagna Z, Troise G, et al. Impact of the improvement of valve area achieved with aortic valve replacement on the regression of left ventricular hypertrophy in patients with pure aortic stenosis. *Ann Thorac Surg*. 2005;79:1291-6; discussion 96.
16. Riess FC, Bader R, Cramer E, Hansen L, Kleijnen B, Wahl G, et al. Hemodynamic performance of the Medtronic Mosaic porcine bioprosthesis up to ten years. *Ann Thorac Surg*. 2007;83:1310-8.

17. Ali A, Halstead JC, Cafferty F, Sharples L, Rose F, Lee E, et al. Early clinical and hemodynamic outcomes after stented and stentless aortic valve replacement: results from a randomized controlled trial. *Ann Thorac Surg*. 2007;83:2162-8.
18. Lehmann S, Walther T, Kempfert J, Leontjev S, Rastan A, Falk V, et al. Stentless versus conventional xenograft aortic valve replacement: midterm results of a prospectively randomized trial. *Ann Thorac Surg*. 2007;84:467-72.
19. Ruel M, Masters RG, Rubens FD, Bedard PJ, Pipe AL, Goldstein WG, et al. Late incidence and determinants of stroke after aortic and mitral valve replacement. *Ann Thorac Surg*. 2004;78:77-83.
20. Hammermeister K, Sethi GK, Henderson WG, Grover FL, Oprian C, Rahimtoola SH. Outcomes 15 years after valve replacement with a mechanical versus a bioprosthetic valve: final report of the Veterans Affairs randomized trial. *J Am Coll Cardiol*. 2000;36:1152-8.